Received: 18 August 2020 | Revised: 5 October 2020 | Accepted: 12 November 2020

DOI: 10.1002/ppap.202000180

FULL PAPER

PLASMA PROCESSES AND POLYMERS

Cold atmospheric plasma jet array for transdermal drug delivery

Yang Lv[1] | Lanlan Nie[1] | Jiangwei Duan[2] | Zhiyu Li[1] | Xinpei Lu[1]

[1]State Key Laboratory of Advanced Electromagnetic Engineering and Technology, School of Electrical and Electronic Engineering, Huazhong University of Science and Technology, Wuhan, China

[2]Jihua laboratory, Guicheng, Nanhai, Foshan, China

Correspondence

Lanlan Nie, Jiangwei Duan, and Xinpei Lu, State Key Laboratory of Advanced Electromagnetic Engineering and Technology, School of Electrical and Electronic Engineering, Huazhong University of Science and Technology, 430074 Wuhan, China.

Email: nielanlan2017@163.com; duanjiangwei@foxmail.com and luxinpei@hotmail.com

Funding information

National Natural Science Foundation of China, Grant/Award Numbers: 11805075, 51625701, 51977096

Abstract

Transdermal drug delivery (TDD) is an important drug delivery method, and cold atmospheric plasma has been proven its potential as a TDD approach. In this study, a 9-channel plasma jet array was designed to enhance TDD efficiency. The Franz diffusion experiment showed that the TDD efficiency of the drug across the skin was enhanced about 2–110 times after the plasma jet array treatment. The histological analysis showed that the structure of the stratum corneum could be destroyed by the plasma. Further investigations indicated that the reactive oxygen species of the plasma jet play a key role in enhancing TDD efficiency. Our results indicated that the plasma jet array is a potential and effective TDD approach.

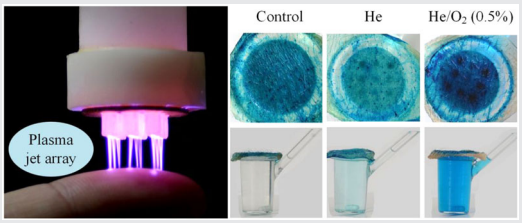

KEYWORDS

cold plasma, histological analysis, jet array, reactive species, transdermal drug delivery

1 | INTRODUCTION

The transdermal drug delivery (TDD) system is non-invasive approach of drug delivery through the skin to the blood circulation. Compared with oral administration and hypodermic injections, the TDD system has so many advantages, such as preventing degradation of the drug by the gastrointestinal tract, avoiding the first-pass effect through the liver, sustaining and controlling drug release, and maintaining the blood drug level so that it becomes a good alternative way of drug delivery.[1–4]

However, it is not easy to get the compounds to enter the internal environment through the skin because of the physiological barrier of the skin. The outermost layer of the skin, the stratum corneum (SC), has a strong barrier function and can block external molecules entering the body, which plays a key role in the barrier effect of the skin.[3] The SC layer is comprised of a matrix of dehydrated and dead corneocytes that are embedded in the mixture of intercellular lipids, and it is often described as having a "brick and mortar" type of structure in which the "bricks" are corneocytes and the mortar is the intercellular lipids.[4,5] Because of the typical components and the tight structure of the SC layer, only a few small molecule drugs with high lipophilicity can naturally permeate through the SC. In other words, hydrophilic

molecules and the molecules with a molecular weight larger than 500 Da can hardly penetrate through the SC layer, which causes a vast majority of drugs to be ruled out for transdermal delivery.[6–8]

To modify the SC layer to change the permeability of the skin, some TDD approaches were developed, such as chemical enhancers,[9] ultrasound,[10] laser,[11] electroporation,[12] microneedle,[13] and thermal ablation,[14] but the drug permeation efficiency, the human body sensitivity, irritation, and patient compliance problems remain to be solved. Thus, new and effective TDD approaches are still needed.[15–17]

The cold atmospheric plasma (CAP) can be a potential effective TDD approach, which is always ignited by the HV at atmospheric pressure and consists of various physical and chemical components, including electrons, ions, neutrals, strong electric field, heat, and ultraviolet light.[18,19] These components may increase the permeability of the skin synthetically. It is reported that the CAP can enhance the TDD efficiency by using plasma jet,[20,21] microplasma,[20] microwave plasma,[22] and air dielectric barrier discharge (DBD) discharge,[23] these reports show that the CAP can modify the skin surface to enhance the permeability of the skin, and the charged particles,[22] power density[23] plays an important role in this process. Nevertheless, its mechanism is not discussed in detail and systematically. Moreover, the stability of the plasma and the size of the treatment area are not well coordinated.

In this study, to explore the potential of CAP in TDD application and uncover the mechanism of CAP for TDD enhancement, a novel helium CAP jet array was designed, which is safe, stable, and has a large treatment area. The temperature of the interface between the plasma jet and the skin was measured. A kind of hydrophilic molecule, patent blue V (MW: 1159.427 Da),[24,25] was used as a model drug for the Franz diffusion TDD test. The histological analysis of the skin was performed to observe the change of epidermal structure after treatment. The contribution of reactive oxygen species (ROS) was investigated. Our results indicated that the CAP jet array is a potential and effective TDD approach and its ROS play a key role in TDD application.

2 | MATERIALS AND METHODS

2.1 | Experimental setup

A double-ring-like electrode[26] with 9-channels DBD plasma jet array was designed in this study, which is presented in Figure 1. The body of the device is made

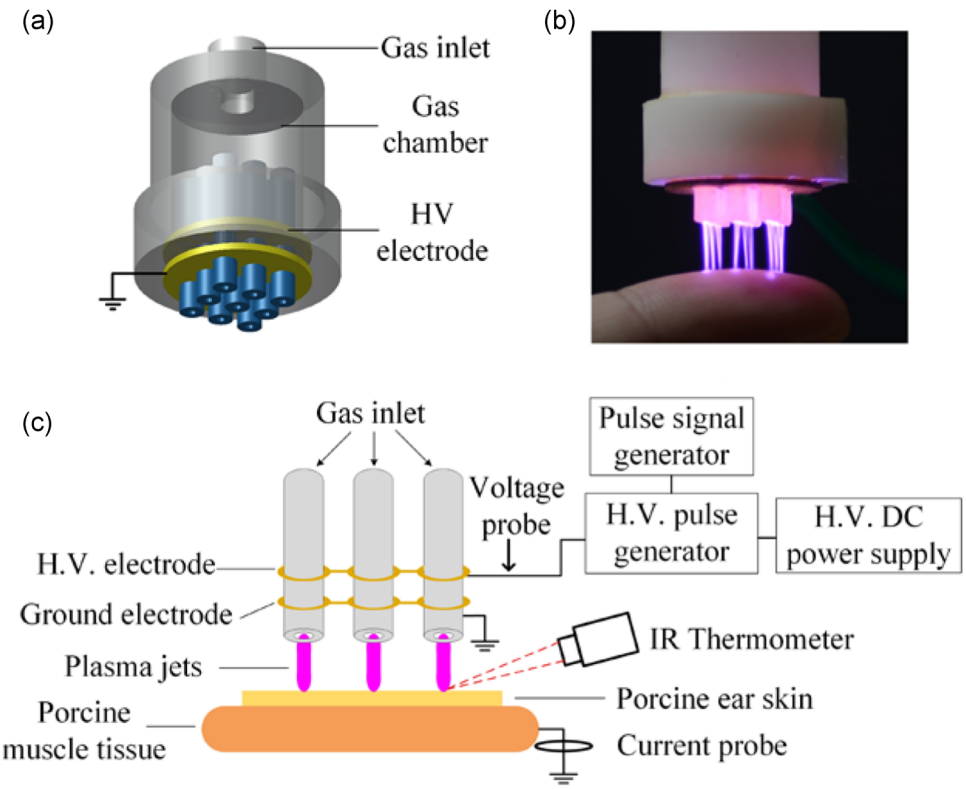

FIGURE 1 (a) Structure of the plasma jet array electrodes. (b) Photograph of the plasma jet array treating human finger. (c) The experimental setup for plasma jet treatment

of resin and the electrode is a couple of copper plates sandwiching the 3-mm thick resin barrier. The high voltage (HV) electrode is isolated with epoxy resin and the electrode on the bottom is connected to the ground. The distance between the grounded electrode and nozzle is 5 mm. The inner and outer diameters of the tube are 1 and 4 mm, respectively (Figure 1a). Figure 1b shows the discharge photo of the plasma jet array; at a certain discharge parameter, this discharge can be touched without electric shock and heat.

The experimental setup for porcine ear skin treatment is presented in Figure 1c. Positive pulsed direct current voltage was applied to drive the jet, the voltage parameters are 7 kV 7 kHz, and the pulse duration was fixed at 1 μs under which the human body can touch the plasma without any heat and electric shock. For further study on the heating effect, 9 kV 9 kHz was chosen because the human body can feel the heat when being touched by the 9 kV 9 kHz drive plasma jets. To explore what role the ROS play in the TDD efficiency enhancement by the plasma jet, two kinds of working gases were used: pure helium or helium mixed with 0.5% oxygen; the total flow rate was controlled by the mass-flow controllers at 5 slm. The gap distance between the tube exit and skin surface was fixed at 3 mm and the treatment time was set at 1.5, 3, or 6 min. Pig muscle tissue was placed under the skin sample during plasma treatment to imitate the real therapeutic state.

The voltage was detected by an HV probe (P6105A; Tektronix), and the discharge current was detected by a current probe (TCP202; Tektronix). The temperature of the interface between plasma jet and the skin during the treatment was detected by an infrared thermometer (OPTCTLL TCF3).

2.2 | Skin preparation

The full-thickness porcine ear skin was obtained freshly from the slaughterhouse; excess subcutaneous fat and connective tissue were carefully removed immediately, then the skin was stored at −20°C for use. The samples were immersed in phosphate-buffered saline (PBS, pH 7.4) for an hour and then wiped dry with absorbent paper before plasma treatment.

2.3 | TDD test

The schematic of the TDD test is shown in Figure 2a and the photos of some experiment groups after 20 h TDD test are shown in Figures 2a and 2d. A system employing Franz diffusion cells with a diffusion area of 2.8 cm^2 was used for the experiment. The receptor phase containing 6.5 ml of PBS was maintained and at 37 ± 1°C under constant stirring at 600 rpm with a magnetic stirrer throughout the experiment. Patent blue V powder was dissolved in fresh PBS to make 12.5 mg/ml patent blue V solution[22]; 2 ml patent blue V solution was added into the donor part during the TDD test. Skin samples were sandwiched between donor and receptor part right after plasma treatment. A total of 200 μl liquid sample was taken out from the receptor part for detection and replaced by equivalent fresh PBS every time during sampling. The concentration of patent blue V in the liquid sample was detected by a microplate reader using the light absorption mode at the wavelength of 636 nm.

2.4 | Histological analysis

Skin samples were exposed to patent blue V solution for 15 min right after plasma treatment to identify the

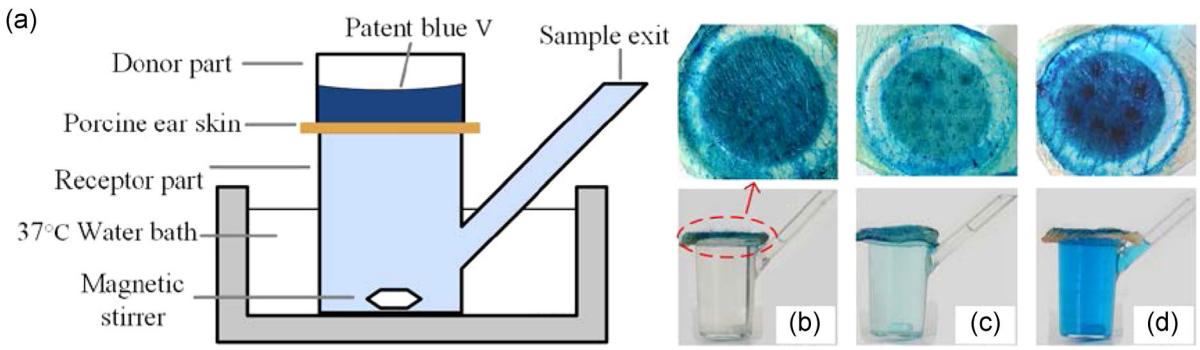

FIGURE 2 (a) The schematic of transdermal drug delivery (TDD) test. (b) Control group after 20 h patent blue V TDD test. (c) Experimental group after 20 h patent blue V TDD test, 7 kV 7 kHz He plasma with 6 min treatment time. (d) Experimental group after 20 h patent blue V TDD test, 7 kV 7 kHz He/O_2(0.5%) plasma with 6 min treatment time. The darker blue 3 × 3 dot matrix on the skin in (c) and (d) is the plasma treatment area.

treated area.[27] Then, the treated area of the skin samples was cut carefully and fixed in 4% paraformaldehyde solution for 24 h; then they were embedded in paraffin and sliced into a 5-μm histological section. After that, the sections were deparaffinized and decolorization then under the hematoxylin and eosin stain.

2.5 | Total ROS flux measurement in the liquid phase

The total ROS generated by plasma–liquid interaction can be measured using 2,7-dichlorodihydrfluorecein (DCFH-DA) due to the fluorescent product, which is named DCF, of oxidation of DCFH generated by the hydrolysis of DCFH-DA.[28] The level of ROS can be estimated by detecting the fluorescence of DCF. The preparation of DCFH-DA solution is described in the report,[29] 2 mM DCFH-DA ethanol solution is prepared and stored at −20°C for use, 500 μl of stock of DCFH-DA was dissolved in 2 ml 10 mM NaOH for 30 min ester hydrolysis at room temperature. Then, the DCFH solution was tested at an excitation wavelength of 485 nm and an emission wavelength of 520 nm, after 3 or 6 min plasma treatment.

3 | RESULTS AND DISCUSSIONS

3.1 | Discharge characteristics of the plasma jet array

The waveforms of voltage and discharge current of this plasma jet array are shown in Figure 3. The discharge mode is similar to a single tube bipolar helium DBD plasma jet, a positive and a negative discharge occur in sequence in every period; it can be found that the discharge of this jet array is stable. The peak value, effective value (root mean square [RMS]), and discharge power are shown in Table 1; the RMS value I_{rms} was calculated using Equation (1) and the discharge power was estimated by Equation (2).

TABLE 1 Peak and effective value of the discharge current and discharge power of the plasma jets

	I_{peak} (mA)		I_{rms} (mA)	Discharge power (W)
7 kV 7 kHz He	320	−420	10.50	1.28
7 kV 7 kHz He/O_2 (0.5%)	260	−370	8.05	0.76
9 kV 9 kHz He	750	−940	21.5	3.73
9 kV 9 kHz He/O_2 (0.5%)	890	−910	20.4	2.38

$$I_{rms} = \sqrt[2]{\frac{\int_0^T i^2 dt}{T}}, \tag{1}$$

$$P = \frac{\int_0^T uidt}{T}, \tag{2}$$

where i is the instantaneous value of the discharge current, u is the instantaneous value of the applied voltage, and T is the period of the applied voltage.

When the applied voltage is 7 kV 7 kHz, though the absolute value of peak current is around 260–420 mA, the RMS value of discharge current is 8–11 mA and the discharge power is 0.7–1.3 W, due to the short current duration, which is less than 100 ns; the human body can touch the plasma jet safely without electric shock and heat. As the applied voltage increase to 9 kV 9 kHz, the peak value of discharge current is increased by 2–3 times, and the RMS

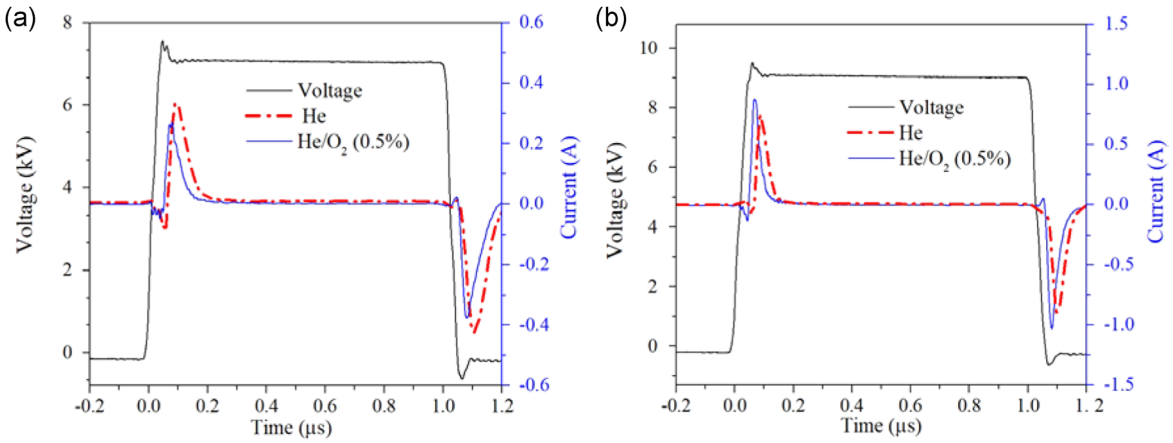

FIGURE 3 Voltage and discharge current under (a) 7 kV 7 kHz and (b) 9 kV 9 kHz power supply

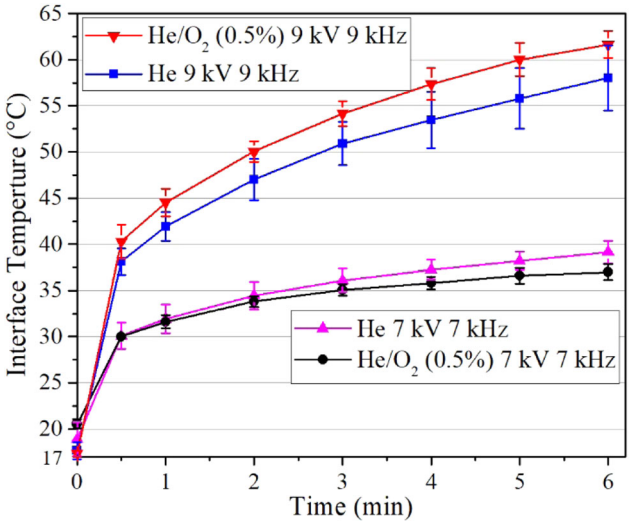

FIGURE 4 Temperature of the interface between the plasma jet and the skin during plasma treatment. The error bars indicate standard errors ($n \geq 3$)

value is up to 20 mA, the discharge power is 3–4 times higher than 7 kV 7 kHz and overheat occurred when the human body touched the plasma jets. The mixing of 0.5% O_2 decreased the discharge power, that may due to the high-electron affinity of the O_2 species which decrease the electron density and caused the decrease of conductivity of the dark channel behind the plasma bullet,[30] decreased the effective value of discharge current which is positively correlated with discharge power (formula 2.2). The results indicate that the discharge current and power of the plasma jet array under 7 kV 7 kHz is so small that it will not cause any electric shock; there is no need to worried about electrical safety.

3.2 | Interface temperature between the plasma jet and the skin

Considering the heat produced by the plasma may affect the TDD efficiency, we detected the interface temperature between plasma and skin temperature during plasma treatment at different treatment conditions; the results are presented in Figure 4. As we can see, the temperature during plasma treatment at the same time depends on the applied voltage; as the treatment time increase, the temperature will increase more and more slowly. When the applied voltage is 7 kV 7 kHz and the treatment time is 6 min, the interface is 35–40°C, which is very close to the human body temperature and cannot cause heating; there is no need to consider the thermal effect of the plasma jet.

Nevertheless, the thermal effect is one of the effective approaches to enhance TDD, which is generally produced by the laser, thermal ablation, and ultrasound.[31] When the applied voltage increased to 9 kV 9 kHz, the plasma jet overheated the interface, and the temperature increased to 60°C.

The results prove that the plasma jet array under 7 kV 7 kHz treatment cannot generate an obvious heating effect on the skin, while the 9 kV 9 kHz plasma jet array can.

3.3 | Patent blue V TDD test

TDD test was operated to explore the permeation of the drug through the plasma-treated skin. Figure 5 shows the results of the patent blue V TDD test and the 20 h TDD data was counted in Table 2. The patent blue V is hard to get into the receptor part through the untreated skin;

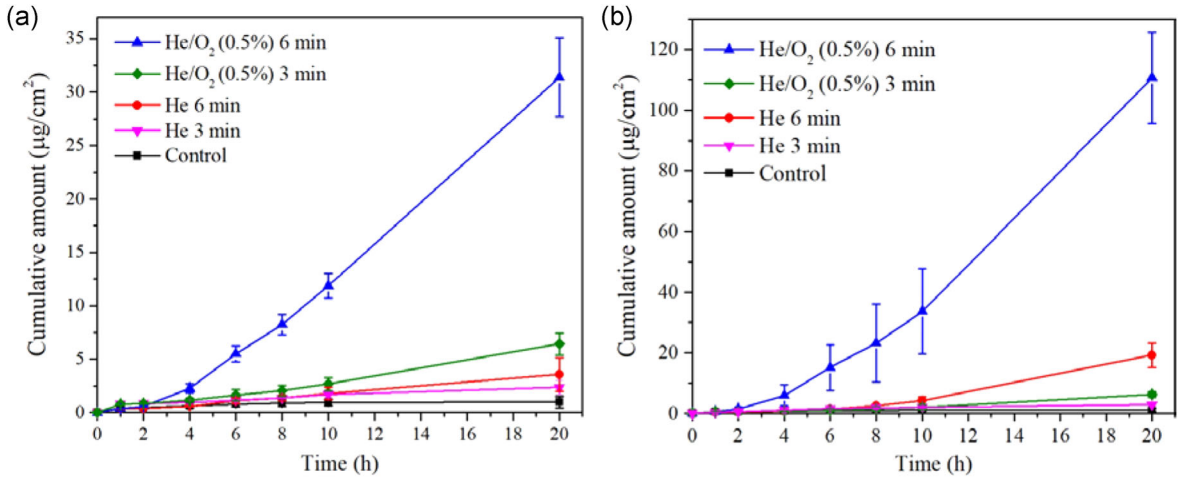

FIGURE 5 Patent blue V permeation cumulative amount through skin sample (a) under 7 kV 7 kHz plasma jet treatment, (b) under 9 kV 9 kHz plasma jet treatment. The error bars indicate standard errors ($n \geq 3$)

TABLE 2 The average penetration cumulative amount of patent blue V after 20 h (μg/cm^2)

Applied voltage		7 kV 7 kHz		9 kV 9 kHz	
Treatment time	Control	3 min	6 min	3 min	6 min
He	1.05	2.35	3.56	2.88	19.15
He/O_2 (0.5%)		6.43	31.39	6.18	110.75

only 1.05 μg/cm^2 cumulative amount was detected after 20 h permeation because its molecule is hydrophilic and molecular weight is 1159.427 Da, larger than 500 Da. For 7 kV 7 kHz applied voltage, as shown in Table 2, the penetration efficiency had a small increase when the working gas was pure He, even with 6 min treatment. When the 0.5% O_2 was mixed into the working gas, the penetration efficiency was 31.39 μg/cm^2, approximately seven times higher than that of pure helium with the same treatment time of 6 min. The mixing of O_2 is so effective that even the 3 min He/O_2 (0.5%) plasma treatment group (6.43 μg/cm^2) is higher than the 6 min pure helium plasma treatment group (3.56 μg/cm^2). For the time variables, as the treatment time increased from 3 to 6 min, there was a small increase in the pure He group but the He/O_2 (0.5%) group had increased by nearly four times. These results indicated that the TDD efficiency of the plasma jet array improved significantly when the 0.5% O_2 is mixed with the working gas, which is related to more ROS generated by the plasma, as reports indicated that the density of the ROS generated by the plasma increase when some oxygen is mixed into the working gas.[32–35]

As the applied voltage increased to 9 kV 9 kHz, compared with 7 kV 7 kHz group, the TDD efficiency was not changed significantly after 3 min treatment, while 6 min treatment increased significantly, which shows that the plasma jet has a cumulative effect on enhancing TDD efficiency. The mixing of O_2 still plays an important role so that the efficiency of 6 min 7 kV 7 kHz He/O_2 mixture group is higher than 6 min 9 kV 9 kHz pure helium group.

These results show that the potential of the plasma jet array in TDD application, under 7 kV 7 kHz with the He/O_2 (0.5%) mixture, is an effective and mild parameter for use, and the enhancement effect on drug penetration increases with time. Increasing the voltage parameters can introduce a thermal effect to enhance the drug penetration efficiency, but overheating may cause unwanted skin damage[36] so the heating time should be well controlled when using it. In the previous study, the SC became thinner or even disappeared after the plasma treatment, which led to the weakening of the barrier function of the skin;[19] the structure change of the skin after plasma jet array treatment is discussed in the next section.

3.4 | Changes in skin structure after plasma treatment

Histological analyses were performed to investigate the structural changes of the skin after plasma treatment. Figure 6 shows the cross-sections of skin sample under 7 kV 7 kHz pure helium and He/O_2 (0.5%) plasma jet treatment. When the working gas is pure helium, after 1.5 min treatment, there was no obvious change on the SC layer (Figure 6b); as the treatment time was increased to 3 min, the SC layer got thinner within around 1.2 mm of the treatment center, but the SC was still continuous (Figure 6c). When the treatment time was increased to 6 min, it showed that the SC layer became much thinner within around 1.5 mm of the treatment center and the SC was exfoliated in an area about 800 mm in diameter (Figure 6d). When the working gas is helium and 0.5% oxygen mixture, the structure of SC had become thinner after 1.5 min treatment within the diameter of 960 μm with the SC was still continuous (Figure 6e); as the treatment time increased to 3 min, the SC became much thinner within 1.5 mm diameter area and 820 μm SC was exfoliated (Figure 6f); as the treatment time up to 6 min, 1.5 mm diameter SC was affected and most SC in that area was exfoliated (Figure 6g). It can be seen in Figure 6g that when the skin is treated by He/O_2 (0.5%) plasma for 6 min, the shallow layer of the viable epidermis in the 100-mm diameter area has been affected. These results show that a plasma jet array under 7 kV 7 kHz has an interactive area with a diameter of about 1.5 mm. In this area, almost all the SC get thinner in varying degrees, and the central area is more serious. From the interactive center, as the time increases, the SC is exfoliated and the exfoliated area gets larger.

Figure 7 shows the cross-sections of skin sample under 9 kV 9 kHz pure helium and He/O_2 (0.5%) plasma jet treatment. When the working gas is pure helium, after 6 min plasma treatment, the 1.5-mm diameter SC was exfoliated and the surface of the viable epidermis in that area has been affected and started to become rough (Figure 7a). When the working gas was He/O_2 (0.5%) mixture, after 6 min, the diameter of exfoliated SC was increased to approximately 2.5 mm and the viable epidermis in that area was damaged to varying degrees; however, the viable epidermis was still continuous (Figure 7b).

These results show that the plasma jet has an etching effect on the SC layer. The etching effect depends on the O_2 mixing, treatment time, and applied voltage, which also affects the TDD efficiency. The results also show that the plasma under 7 kV 7 kHz

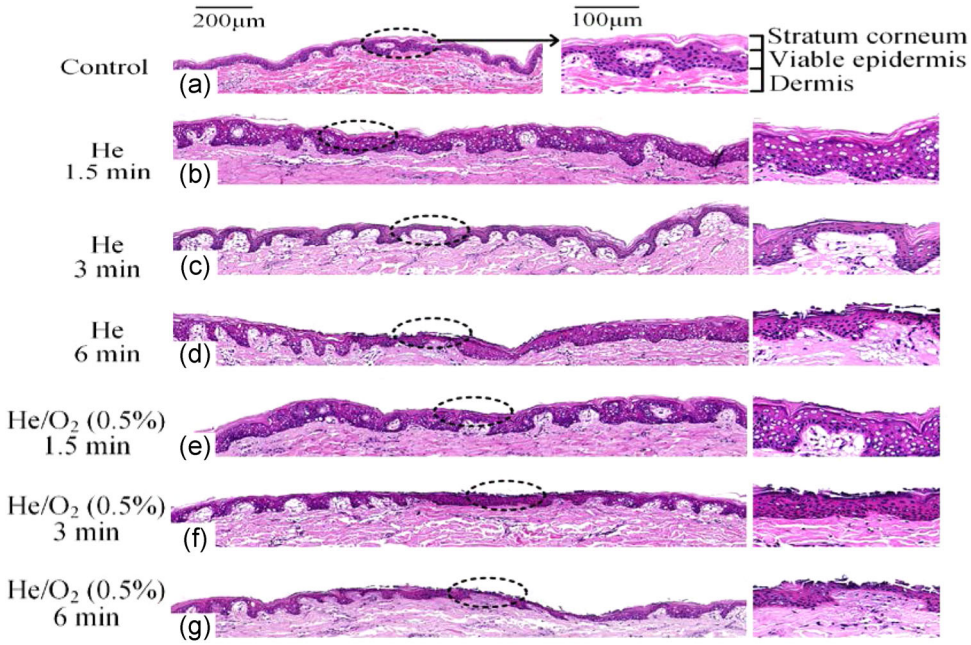

FIGURE 6 Hematoxylin- and eosin-stained cross-sections of skin samples (a) without treatment, under 7 kV 7 kHz applied voltage with (b) 1.5 min He plasma treatment, (c) 3 min He plasma treatment, (d) 6 min He plasma treatment, (e) 1.5 min He/O_2 (0.5%) mixture plasma treatment, (f) 3 min He/O_2 (0.5%) mixture plasma treatment, and (f) 6 min He/O_2 (0.5%) mixture plasma treatment. The circled area is the most severely damaged location, and its higher magnification image is on the right

with He/O_2 (0.5%) as working gas has a higher etching effect on the SC and less damage to the viable epidermis, which is mild and effective for clinical use.

3.5 | The effect of ROS on TDD efficiency

Considering that the TDD efficiency is significantly enhanced when the working gas is mixed with 0.5% O_2 (Figure 6), and the fact that the density of the ROS generated by the plasma increase when some oxygen is mixed with the working gas,[32] we infer that the ROS generated by the plasma play a key role in TDD efficiency enhancement. Later, we measured the total ROS generated by the plasma jet array.

Figure 8a shows the data of relative ROS flux, and the patent blue V penetration cumulative amount after 20 h was recorded in Figure 8b. As we can see, the ROS flux increase with the treatment time and the 0.5% O_2 mixing. Comparing Figure 8a,b the cumulative amount of drug penetration after 20 h is increased with the ROS flux. Therefore, it can be concluded that the density of the total ROS flux in the plasma jet is positively correlated with drug percutaneous penetration efficiency; the ROS play an important role in changing skin permeability.

As reported by van der Paal et al.,[37] the ROS generated by the plasma could pass through cell membranes, which contain unsaturated lipids or cholesterol. The dead keratinocytes and lipid matrix of SC contain abundant unsaturated lipids and cholesterol. On the one hand, the ROS produced by the plasma jets may oxidize

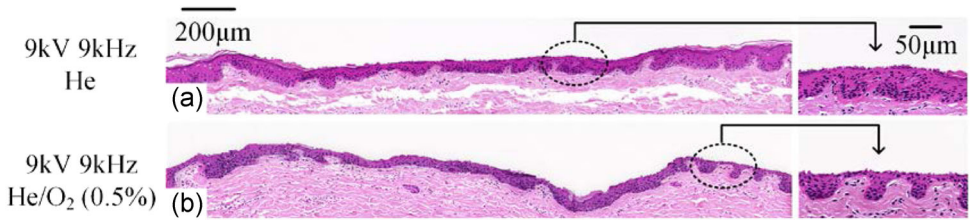

FIGURE 7 Hematoxylin- and eosin-stained cross-sections of 9 kV 9 kHz (a) He plasma and (b) He/O_2 mixture plasma treatment for 6 min. The circled area is the most severely damaged location, and its higher magnification image is on the right

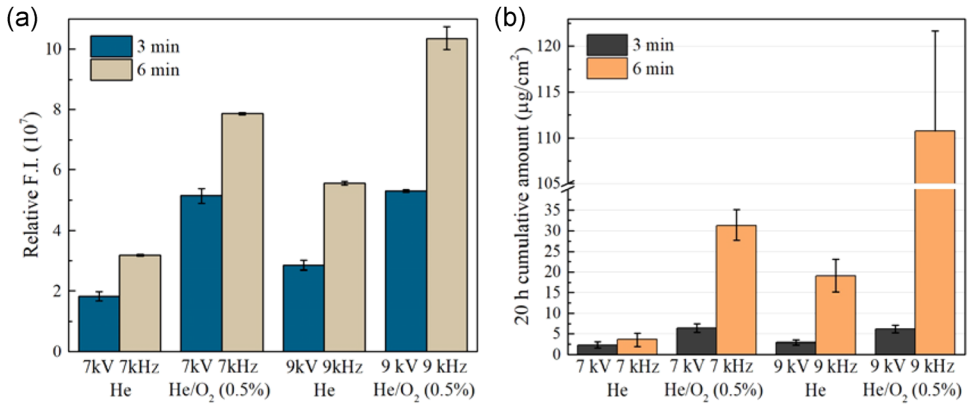

FIGURE 8 (a) The relative density of total reactive oxygen species, (b) penetration cumulative amount of patent blue V after 20 h, under different treatment conditions. The error bars indicate standard errors ($n \geq 3$)

the unsaturated lipids in the cell membrane or passively diffuse into the cells to react with the organic molecules (amino acids or the lipids[38–40]; on the other, the ROS may oxidize the intercellular lipid matrix, resulting in the instability of the structure due to the presence of unsaturated lipids or cholesterol causing the etching effect on SC and increase the permeability of the skin.

4 | CONCLUSION

A novel plasma jet array as a treatment source with adjustable dose was reported for the TDD, which can have better patient compliance and higher drug penetration efficiency. The plasma jets generated by this device can be touched by the human body without any electric shock and heat. The patent blue V TDD Franz diffusion experiment results showed that the TDD efficiency of a drug across the skin was enhanced about 2–110 times after the plasma jet array treatment, which indicated that the plasma jet array has an ideal TDD efficiency enhancement and the potential of plasma jet array on the TDD. The results of histological analyses have shown that the plasma has an etching effect on the epidermis, and the etching effect can be controlled by treatment time, power supply, and O_2 mixture. The thermal effect can be used as a selectable factor for TDD by controlling the supplied power. The flux of ROS can be significantly increased by mixing a small amount of oxygen, which plays a key role in the TDD process.

Nowadays, the painless and nonirritating way of etching SC is needed in many clinical applications; this article is not only aimed at the enhancement of TDD by CAP but also provides a certain reference value for the study of the interaction between cold atmospheric plasma and the skin.

ACKNOWLEDGMENTS

This study was partially supported by the National Natural Science Foundation of China (Grant Nos: 51625701, 51977096, and 11805075).

ORCID

Lanlan Nie https://orcid.org/0000-0002-1680-2775
Jiangwei Duan https://orcid.org/0000-0003-1213-2804
Xinpei Lu https://orcid.org/0000-0003-0676-9585

REFERENCES

[1] M. R. Prausnitz, R. Langer, *Nat. Biotechnol.* **2008**, *11*, 1261.
[2] H. Marwah, T. Garg, A. K. Goyal, G. Rath, *Drug Delivery* **2016**, *2*, 564.
[3] G. K. Menon, G. W. Cleary, M. E. Lane, *Int. J. Pharm.* **2012**, *435*, 3.
[4] J. van Smeden, M. Janssens, G. S. Gooris, J. A. Bouwstra, *Biochim. Biophys. Acta, Mol. Cell Biol. Lipids* **2014**, *1841*, 295.
[5] P. M. Elias, *J. Invest. Dermatol.* **1983**, *80*, 44s.
[6] H. Lee, C. Song, S. Baik, D. Kim, T. Hyeon, D.-H. Kim, *Adv. Drug Delivery Rev.* **2018**, *127*, 35.
[7] J. D. Bos, M. M. H. M. Meinardi, *Exp. Dermatol.* **2000**, *9*, 165.
[8] M. R. Prausnitz, S. Mitragotri, R. Langer, *Nat. Rev. Drug Discovery* **2004**, *3*, 115.
[9] Y. Chen, P. Quan, X. Liu, M. Wang, L. Fang, *Asian J. Pharm. Sci.* **2014**, *9*, 51.
[10] B. E. Polat, D. Hart, R. Langer, D. Blankschtein, *J. Controlled Release* **2011**, *152*, 330.
[11] M. Park, H. Jang, F. V. Sirotkin, J. J. Yoh, *Opt. Lett.* **2012**, *37*, 3894.
[12] N. A. Charoo, Z. Rahman, M. A. Repka, S. N. Murthy, *Curr. Drug Delivery* **2010**, *7*, 125.
[13] S. H. Bariya, M. C. Gohel, T. A. Mehta, O. P. Sharma, *J. Pharm. Pharmacol.* **2011**, *64*, 11.
[14] R. Parhi, A. Mandru, *Drug Delivery Transl. Res.* **2020**, https://doi.org/10.1007/s13346-020-00823-3
[15] Y. Zhang, J. Yu, A. R. Kahkoska, J. Wang, J. B. Busec, Z. Gu, *Adv. Drug Delivery Rev.* **2019**, *139*, 51.
[16] X. He, J. Sun, J. Zhuang, H. Xu, D. Wu, *Dose–Response* **2019**, *4*, 155932581987858.

[17] Q. Pan, Y. Yu, D. Chen, G. Jiao, X. Liu, *Front. Chem. Sci. Eng.* **2020**, *14*, 378.
[18] X. Lu, M. Keidar, M. Laroussi, E. Choi, E. J. Szili, K. Ostrikov, *Mater. Sci. Eng. R* **2019**, *138*, 36.
[19] M. He, J. Duan, J. Xu, M. Ma, B. Chai, G. He, L. Gan, S. Zhang, X. Duan, X. Lu, H. Chen, *Plasma Processes Polym.* **2020**, *17*, e1900068.
[20] K. Shimizu, N. A. Tran, K. Hayashida, M. Blajan, *J. Phys. D: Appl. Phys.* **2016**, *49*, 315201.
[21] O. Lademann, H. Richter, A. Kramer, A. Patzelt, M. C. Meinke, C. Graf, Q. Gao, E. Korotianskiy, E. Rühl, K.-D. Weltmann, J. Lademann, S. Koch, *Laser Phys. Lett.* **2011**, *8*, 758.
[22] H. Y. Lee, J. H. Choi, J. W. Hong, G. C. Kim, H. J. Lee, *J. Phys. D: Appl. Phys.* **2018**, *51*, 215401.
[23] M. Gelker, C. C. Müller-Goymann, W. Viöl, *Skin Pharmacol. Physiol.* **2020**, *33*, 1.
[24] B. Zorec, J. Jelenc, D. Miklavčič, N. Pavšelj, *IFMBE. Proc.* **2016**, *57*, 1030.
[25] M. L. Yarmush, A. Golberg, G. Serša, T. Kotnik, D. Miklavčič, *Annu. Rev. Biomed. Eng.* **2014**, *16*, 295.
[26] M. Laroussi, C. Tendero, X. Lu, S. Alla, W. Hynes, *Plasma Processes Polym.* **2006**, *3*, 470.
[27] D. F. S. Fonseca, P. C. Costa, I. F. Almeida, P. Dias-Pereira, I. Correia-Sá, V. Bastos, H. Oliveira, M. Duarte-Araújo, M. Morato, C. Vilela, A. J. D. Silvestre, C. S. R. Freire, *Carbohydr. Polym.* **2020**, *241*, 116314.
[28] E. J. Szili, J.-S. Oh, H. Fukuhara, R. Bhatia, N. Gaur, C. K. Nguyen, S.-H. Hong, S. Ito, K. Ogawa, C. Kawada, T. Shuin, M. Tsuda, M. Furihata, A. Kurabayashi, H. Furuta, M. Ito, K. Inoue, A. Hatta, R. D. Short, *Plasma Sources Sci. Technol.* **2018**, *27*, 014001.
[29] Y. Yang, Z. Li, L. Nie, X. Lu, *J. Appl. Phys.* **2019**, *125*, 223302.
[30] Y. Xian, P. Zhang, X. Pei, X. Lu, *IEEE Trans. Plasma Sci.* **2014**, *42*, 2448.
[31] A. Aharon, K. Luai, E. Giora, K. Joseph, *Adv. Drug Delivery Rev.* **2014**, *72*, 127.
[32] E. Takai, T. Kitamura, J. Kuwabara, S. Ikawa, S. Yoshizawa, K. Shiraki, H. Kawasaki, R. Arakawa, K. Kitano, *J. Appl. Phys.* **2014**, *47*, 285403.
[33] A. M. Lietz, M. J. Kushner, *J. Appl. Phys.* **2018**, *124*, 153303.
[34] N. Knake, S. Reuter, K. Niemi, V. Schulz-von der Gathen, J. Winter, *J. Phys. D: Appl. Phys.* **2008**, *41*, 194006.
[35] G. Park, H. Lee, G. Kim, J. K. Lee, *Plasma Processes Polym.* **2008**, *5*, 569.
[36] S. Kos, T. Blagus, M. Cemazar, G. Filipic, G. Sersa, U. Cvelbar, *PLoS One* **2017**, *12*, e0174966.
[37] J. van der Paal, S.-H. Hong, M. Yusupov, N. Gaur, J.-S. Oh, R. D. Short, E. J. Szili, A. Bogaerts, *Phys. Chem. Chem. Phys.* **2019**, *21*, 19327.
[38] M. Gavahian, Y.-H. Chu, A. M. Khaneghah, F. J. Barba, N. N. Misra, *Trends Food Sci. Technol.* **2018**, *77*, 32.
[39] J. Duan, M. Ma, M. Yusupov, R. M. Cordeiro, X. Lu, A. Bogaerts, *Plasma Processes Polym.* **2020**, *17*, e2000005.
[40] J. V. der Paal, S. Aernouts, A. C. T. van Duin, E. C. Neyts, A. Bogaerts, *J. Phys. D: Appl. Phys.* **2013**, *46*, 395201.

How to cite this article: Lv Y, Nie L, Duan J, Li Z, Lu X. Cold atmospheric plasma jet array for transdermal drug delivery. *Plasma Process Polym*. 2020;e2000180.
https://doi.org/10.1002/ppap.202000180